

## CHARACTERISTICS AND REDUCIBILITY OF NANOSIZED $\text{La}_{1-x}\text{Ce}_x\text{CoO}_3$ PEROVSKITES SYNTHESIZED BY REACTIVE GRINDING

Received 7 June 2008

NGUYEN TIEN THAO<sup>1</sup>, NGO THI THUAN<sup>1</sup>, SERGE KALIAGUINE<sup>2</sup>

<sup>1</sup> Faculty of Chemistry, College of Sciences, Vietnam National University, Hanoi

<sup>2</sup> Department of Chemical Engineering, Laval University, Canada. G1K 7P4.

### ABSTRACT

Two  $(\text{La,Ce})\text{CoO}_3$  perovskite-type oxides prepared by reactive grinding have been characterized by means of X-ray diffraction,  $\text{N}_2$  adsorption/desorption isotherms, SEM,  $\text{H}_2$ -TPR. Both samples show a nanocrystalline phase and rather high surface area. The thermal stability of cobalt ions in such solids has been studied under reducing conditions.  $\text{H}_2$ -TPR results indicate that the reduction of  $\text{Co}^{3+}$  to  $\text{Co}^0$  occurs in a multiple-step. The partial replacement of  $\text{La}^{3+}$  by  $\text{Ce}^{4+}$  has promoting effects on the reducibility of cobalt ions. A decreased reduction temperature of cobalt ions in the presence of  $\text{Ce}^{4+}$  leads to an increased dispersion of the reduced phase for  $\text{La}_{0.9}\text{Ce}_{0.1}\text{CoO}_3$  perovskite precursor.

**Keywords:** perovskite; reduction; cobalt; La-Ce-Co; dispersion; metal.

### I - INTRODUCTION

Perovskite-type oxides with the general formula  $\text{ABO}_3$  have been much paid special attention for the last three decades due to their potential applications in catalysis and pollutant elimination [1]. For example, some perovskites such as  $\text{LaCoO}_3$ ,  $\text{LaMnO}_3$ ,  $\text{LaCrO}_3$  have been used in environmental catalysis reactions including CO oxidation, methane combustion,  $\text{NO}_x$  decomposition, and exhaust treatment [1-2]. However, these applications are mainly based on the electronic configuration of the  $\text{B}^{3+}$  cations. In recent years, there has been an interest in using mixed-oxide type perovskites  $\text{Ln}(\text{Co,Fe, Ni, Cu})\text{O}_3$  as prominent precursors for preparation of a "metal on oxide" solid [3-5]. Because of the complexity of perovskite system which often contains mixed valence ions and variable stoichiometry, a transition metal

with lower oxidation states could exhibit numerous different kinds of catalytic sites active for several reactions when pre-treated under tailored conditions [4 - 6]. For example, the reduction of  $\text{La}(\text{Co,Fe,Ni,Cu})\text{O}_3$  perovskites at high temperature leads to the formation of a blend of metals, alloys, ions. [3 - 6]. The reduced phase was reported to be very active for hydrogenation of ethylene [7], reforming of  $\text{CO}_2$  [4], Fischer-Tropsch synthesis [3], alcohol synthesis [5, 8, 9]. In some ways, the incomplete reduction of perovskite results in the formation of the intermediates of transition metals and the homogeneity of active sites on the catalyst surface which may become a promising the catalytic sites for many appropriate reactions.

This part of the present study is to deal with the reducibility of cobalt ions in two ground perovskites and to pave the way for preparation

of several catalytic systems from the cobaltate perovskite precursors. The next contributions will be concentrated on the applications of the incomplete reduction of  $\text{La}_{1-x}\text{Ce}_x\text{CoO}_3$  perovskites in the epoxidation of styrene and in the hydrogenation of carbon monoxide.

## II - EXPERIMENTAL

$\text{La}_{1-x}\text{Ce}_x\text{CoO}_3$  perovskite-type mixed oxides were synthesized by the reactive grinding method [5, 8, 10]. The stoichiometric proportions of commercial lanthanum, cerium, and cobalt oxides (99%, Aldrich) were mixed together with three hardened steel balls (diameter = 11 mm) in a hardened steel crucible (50 ml). A SPEX high energy ball mill working at 1000 rpm was used for mechano-synthesis. Milling was carried out for 8 hours prior to a second milling step with an alkali additive if used. A sample was added into a beaker containing 1200 mL water and stirred by magnetic stirring for 90 min prior to being sedimented for 3-5 hours. After the clean water is removed, the slurry was dried in oven at 60 - 80°C before calcination at 250°C for 150 min.

The specific surface area of all obtained samples was determined from nitrogen adsorption equilibrium isotherms at -196°C measured using an automated gas sorption system (NOVA 2000; Quantachrome). X-ray diffraction (XRD) was collected using a SIEMENS D5000 diffractometer with  $\text{CuK}\alpha$  radiation ( $\lambda = 1.5406$  nm). Bragg's angles between 20 and 60° were collected at a rate of 1°/min. Average crystal domain sizes ( $D$ ) were

evaluated by means of the Debye-Scherrer equation  $D = K\lambda/\beta\cos\theta$  after Warren's correction for instrumental broadening [11].

SEM images were recorded using a JEOL JSM-840 electron microscope with magnification of 25,000. The acceleration voltage was 10 kV. The samples were dispersed on an aluminum stub and coated with Au//Pt film.

Temperature Programmed Reduction (TPR) experiments were carried out using a multifunctional apparatus (RXM-100 from Advanced Scientific Designs, Inc.). Prior to each TPR analysis, a 50 mg sample was calcined at 500°C for 90 min under flowing 20%  $\text{O}_2/\text{He}$  (20 ml/min, ramp 5°C/min). The sample was then cooled to room temperature under flowing pure He (20 mL/min).  $\text{H}_2$ -TPR of the catalyst was then carried out by ramping under 5 vol% of  $\text{H}_2/\text{Ar}$  (20 ml/min) from room temperature up to 800°C (5°C/min). The hydrogen consumption was determined using a TCD with a reference gas of same composition as the reducing gas ( $\text{H}_2/\text{Ar}$ ).

## III - RESULTS AND DISCUSSION

### 1. Catalyst characteristics

Both the two perovskites were prepared by the reactive method, but NaCl was used as an additive for the preparation of  $\text{LaCoO}_3$  while no additive was introduced during the synthesis step of  $\text{La}_{0.9}\text{Ce}_{0.1}\text{CoO}_3$ . Table 1 summarized several physical properties and preparative conditions of the solids.

Table 1: Physical properties of catalysts

Sample	$T_{\text{cal}}$ (°C)	Crystal domain (nm) <sup>1</sup>	$S_{\text{BET}}$ ( $\text{m}^2/\text{g}$ ) <sup>2</sup>	Pore diameter (nm) <sup>2</sup>	Additive	Impurity
$\text{LaCoO}_3$	250	9.8	56.9	12.7	NaCl	$\text{Co}_3\text{O}_4$
$\text{La}_{0.9}\text{Ce}_{0.1}\text{CoO}_3$	250	10.2	71.0	11.9	non	$\text{La}_2\text{O}_3$ , $\text{Co}_3\text{O}_4$

1: Calculated by the Scherrer equation from X-ray line broadening [11]

2: Determined from  $\text{N}_2$  desorption isotherm.

Table 1 shows that the specific surface area of  $\text{La}_{0.9}\text{Ce}_{0.1}\text{CoO}_3$  sample is rather higher than

that of the cobaltate. Meanwhile no significant difference in diameter of catalyst particles

between the two samples is observed (Table 1). This is consistent with the results of SEM technique. As seen from Figure 1 the catalyst is likely composed of uniform spherical particles. Such particles are further constituted of agglomerates of primary nanometric particles with diameters approximately of 10 nm as estimated from X-ray line broadening using Scherrer equation [9, 11]. The crystal domains

are close to the pore diameter determined from  $N_2$  desorption isotherm, implying that their ground perovskites have somewhat porous structure. The porosity of the ground materials are assumedly built from the spaces of individual elementary nanoparticles. Similar structures were already reported by several groups for nanosized Co-based perovskites using the same preparation method [10, 12].

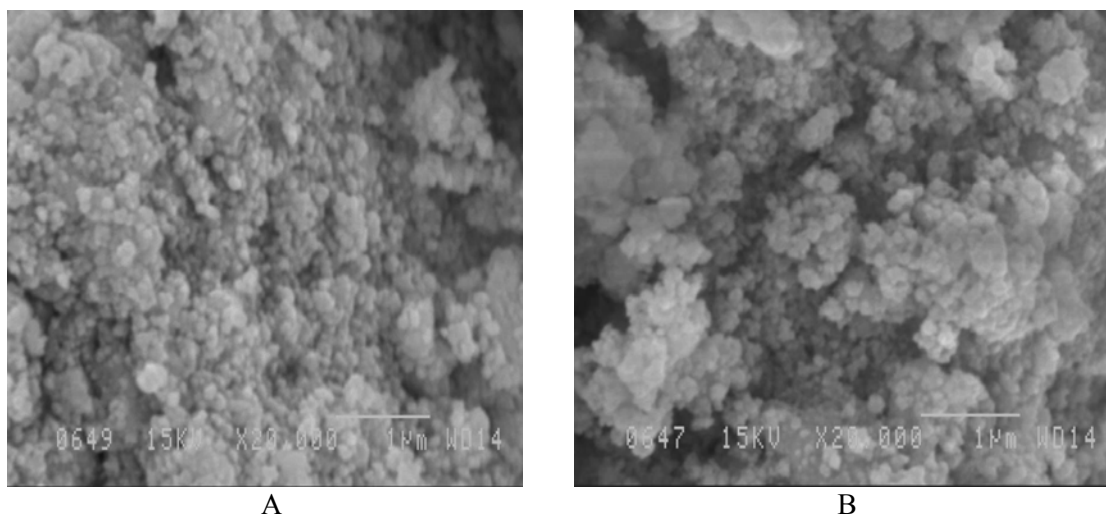


Figure 1: SEM photographs of  $LaCoO_3$  (A) and  $La_{0.9}Ce_{0.1}CoO_3$  (B) nanocrystalline perovskites after calcined at  $250^\circ C$

The crystallite phase identification of the solid solutions was accomplished by mean of XRD. X-ray diffraction spectra of all samples calcined at  $250^\circ C$  are displayed in figure 2. As seen from this figure, both the two ground catalysts show strong reflections of the perovskite phase with the rhombohedral structure. Besides the major phase of perovskites, some minor phases including  $Co_3O_4$  in the case of  $LaCoO_3$  and  $Co_3O_4 + La_2O_3$  in the case of Ce-containing sample were detected (figure 2 and table 1). The perovskite diffraction lines are rather broad, suggesting the formation of a nanophase [10]. This is good harmony with the SEM photographs illustrated in Fig. 1. Because the preparation of such samples is based on the solid-solid reactions between intimate mixtures of the constituent binary oxides ( $La_2O_3$ ,  $Co_3O_4$ ,  $CeO_2$ ) under milling conditions, the products have a limited

degree of chemical homogeneity and usually consist of a small amount of unreacted oxide impurities [1, 5, 8, 10]. Therefore, the presence of  $Co_3O_4$  and  $La_2O_3$  on the ground perovskite surface is understandable. Figure 2 indicates the successful substitution of a small part of  $La^{3+}$  by  $Ce^{4+}$ . No clear signals of  $CeO_x$  are observable for the ground  $(La,Ce)CoO_3$  sample, implying that cerium is mostly in the perovskite structure. No significant change in rhombohedral structure between  $LaCoO_3$  and  $La_{0.9}Ce_{0.1}CoO_3$  perovskites is observed although 10% of the lanthanum in lattice is literally replaced by cerium. In this case, the perovskite structure is still well-preserved.

#### *Reducibility of $La_{1-x}Ce_xCoO_3$ perovskites*

Temperature programmed reduction of hydrogen ( $H_2$ -TPR) was carried out from room temperature to  $800^\circ C$  in order to investigate the

reducibility of the two ground perovskites. H<sub>2</sub>-TPR profiles of such materials displayed Figure 4 present a low-temperature peak at 410°C with a small back-shoulder at 440°C and a higher temperature peak at 705°C for LaCoO<sub>3</sub> [13]. The amount of hydrogen consumed provides evidence of the reduction of Co<sup>3+</sup> in perovskite lattice to Co<sup>2+</sup> at 410°C. After this reduction step, the incompletely reduced Co<sup>2+</sup> ions are assumed to be present in the perovskite framework. The higher temperature peak is ascribed to the reduction of Co<sup>2+</sup> to metallic cobalt accompanied by the collapse of the

perovskite structure. After the complete reduction, metallic cobalt phase is suggested to be very finely dispersed on lanthanum oxide. Meanwhile, H<sub>2</sub>-TPR curve of La<sub>0.9</sub>Ce<sub>0.1</sub>CoO<sub>3</sub> perovskite show three distinct peaks at 310, 370 and 605°C, suggesting the occurrence of a multiple-step reduction. The reduction of Co<sup>3+</sup> in the perovskite lattice to Co<sup>2+</sup> takes place at 310°C. The small shaped-peak at 370°C, likely corresponding to the shoulder at 440°C for H<sub>2</sub>-TPR curve of LaCoO<sub>3</sub>, is assigned to the reduction of the extra-perovskite lattice cobalt (Co<sub>3</sub>O<sub>4</sub>) to lower oxidation states [14].

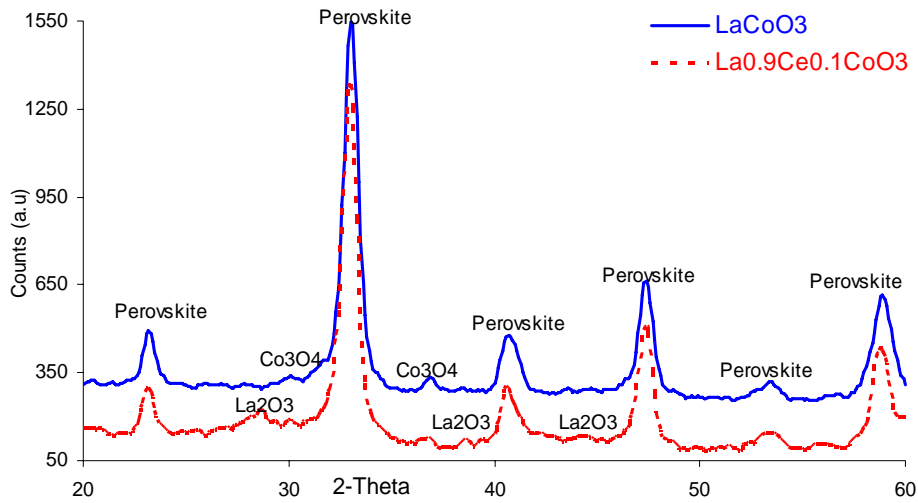


Figure 2: X-ray diffraction patterns of La<sub>1-x</sub>Ce<sub>x</sub>CoO<sub>3</sub>

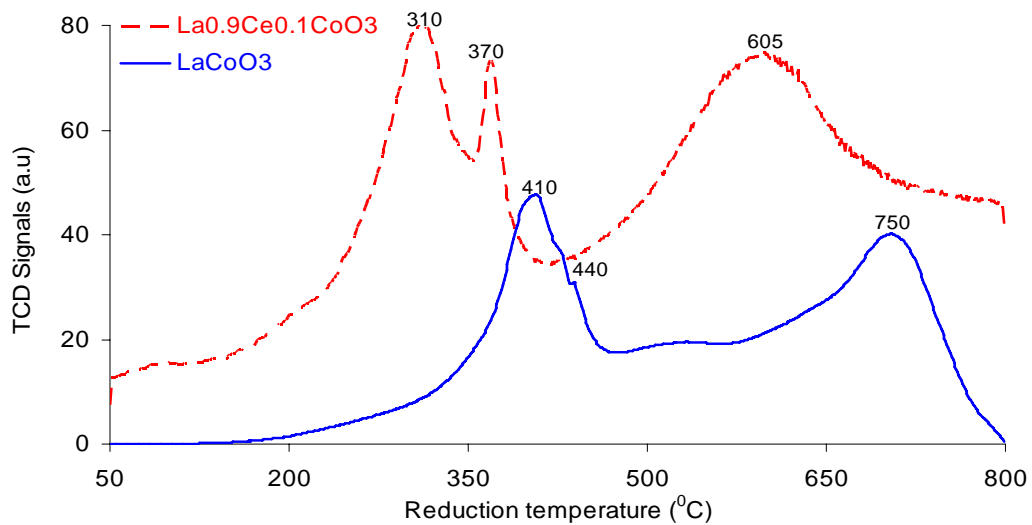


Figure 3: H<sub>2</sub>-TPR of the two ground perovskites

In order to shed in light to this point, X-ray diffraction of both samples reduced at 400°C for 90 min were recorded. Figure 4 shows the presence of the main phase of perovskite with strong reflection intensities, indicating the stable perovskite structure under reduction conditions reported in figure 4. It should be paid attention to the disappearance of small reflections characterizing to the presence of cobalt oxide phase while signals of La<sub>2</sub>O<sub>3</sub> are still detectable as compared with the spectra of their parent samples in figure 2. Instead, the appearance of very weak diffraction lines at 2θ = 44.3 and 51.5° is probably assumed to the formation of tiny metallic cobalt particles (Co) (figure 4). This is good agreement with the results of H<sub>2</sub>-TPR which indicate the reduction of Co<sup>3+</sup> in perovskite lattice and Co<sub>3</sub>O<sub>4</sub> oxide impurities to lower oxidation states at 310 and 370°C (figure 3). The higher temperature peak corresponds to the reduction of Co<sup>2+</sup> in the perovskite intermediate phases of La<sub>0.9</sub>Ce<sub>0.1</sub>CoO<sub>3-x</sub> (x ≤ 2.5) perovskites to Co<sup>0</sup> [13]. The reduction of La<sup>3+</sup> and Ce<sup>4+</sup> in the perovskite lattice likely occurs only at higher temperatures (> 800°C) [15]. It is clearly observed that the reduction temperature of La<sub>0.9</sub>Ce<sub>0.1</sub>CoO<sub>3</sub> systematically shifts to lower temperatures as compared with that of cerium free-perovskite.

Indeed, the presence of Ce<sup>4+</sup> in the perovskite lattice decreases the reduction temperature of Co<sup>3+</sup>. In other words, cerium ions have the promoting effects on cobalt ion reduction. CeO<sub>x</sub> has been thoroughly reported to promote metal oxide reduction for Pd/CeO<sub>2</sub>/Al<sub>2</sub>O<sub>3</sub>, CuMgCeO<sub>x</sub> [16, 17]. The presence of cerium ions may be capable of playing a crucial role in the enhancement of reducibility of cobalt ions via the hydrogen spillover effects [18]. Another explanation may stem from some minor alterations in the perovskite structure. A small difference in the atomic radii and oxidation state between La<sup>3+</sup> with trivalent (r<sub>La</sub> = 1.061 Å) and Ce<sup>4+</sup> with tetravalent (r<sub>Ce</sub> = 1.034 Å) leads to a slightly distorted structure [5, 19]. This modified structure should be less thermal stability than the corresponding perovskite-type cobaltate (LaCoO<sub>3</sub>). In addition, a higher specific surface area of La<sub>0.9</sub>Ce<sub>0.1</sub>CoO<sub>3</sub> is higher than the-one of LaCoO<sub>3</sub> so that the diffusion of hydrogen reactant and the mass transport water product across lattice of the porous and on the external surface of the former (S<sub>BET</sub> = 70 m<sup>2</sup>/g) become much easier than those of the latter (S<sub>BET</sub> = 56 m<sup>2</sup>/g). All these factors make La<sub>0.9</sub>Ce<sub>0.1</sub>CoO<sub>3</sub> perovskite less thermal stability under hydrogen atmosphere as demonstrated in figure 3.

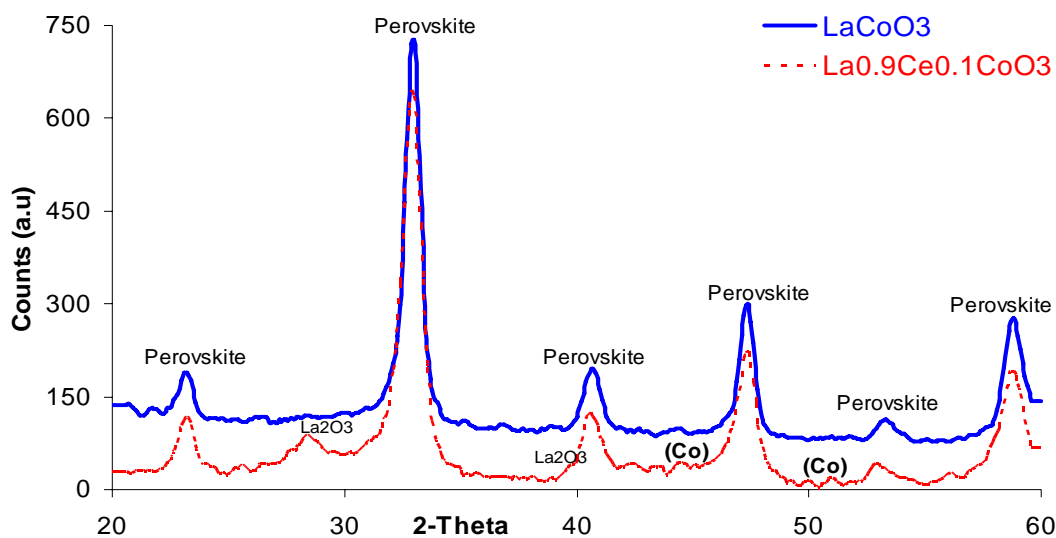


Figure 4: XRD patterns of La<sub>1-x</sub>Ce<sub>x</sub>CoO<sub>3</sub> reduced at 400°C under hydrogen atmosphere for 90 min

Fortunately, the decreased reduction temperature of cobalt ions in  $\text{La}_{0.9}\text{Ce}_{0.1}\text{CoO}_3$  leads to the prevention of the sintering of cobalt atoms in the perovskite lattice. The resultant relevant material may be present in the form of a perovskite-type metallic oxide that is promising catalyst for desirable applications [1, 6, 7, 20].

#### IV - CONCLUSION

Two ground  $\text{La}_{1-x}\text{Ce}_x\text{CoO}_3$  perovskites have been successfully synthesized and characterized. The solid solutions have rather high surface area and consist of elementary nanometric particles. The existence of small spaces between nanoparticles of perovskite makes these ground materials more porous. Under hydrogen atmosphere, the reduction of cobalt ions takes place via two consecutive steps:  $\text{Co}^{3+}/\text{Co}^{2+}$  and  $\text{Co}^{2+}/\text{Co}^0$ . After the first reduction step from  $\text{Co}^{3+}$  to  $\text{Co}^{2+}$ , the perovskite structure is still preserved. The further reduction yields highly dispersed metallic cobalts on  $\text{La}_2\text{O}_3$  matrix. An introduction of  $\text{Ce}^{4+}$  ions into the perovskite lattice has remarkably affected the reducibility of cobalt ions. A substantially decreased reduction temperature of cobalt ions was observed for sample  $\text{La}_{0.9}\text{Ce}_{0.1}\text{CoO}_3$ . Some explanations are suggested to illustrate the effects of  $\text{Ce}^{4+}$  ions in the perovskite lattice on the reducibility of cobalt ions.

**Acknowledgements.** *The financial support by the Natural Science and Engineering Research Council of Canada for the present research is gratefully acknowledged.*

#### REFERENCES

1. M. A. Pena and J. L. G. Fierro. Chem. Rev., 101, 1981 - 2017 (2001).
2. K. Tabata and M. Misono. Catal. Today, 8, 249 - 261 (1990).
3. L. Bedel, A. C. Roger, J. L. Rehspringer, Y. Zimmermann, A. Kiennemann. J. Catal., 235, 279 - 294 (2005).
4. S. M. De Lima, J. M. Assaf. Catal. Letters, 108, 63 - 70 (2006).
5. N. Tien-Thao, H. Alamdari, M. H. Zahedi-Niaki, S. Kaliaguine. Appl. Catal. A 311, 204 - 212 (2006).
6. J. L. G. Fierro, M. A. Pena, L. G. Tejuca. J. Mater. Sci., 23, 1018 - 1023 (1988).
7. J. O. Petunchi, M. A. Ulla, J. A. Marcos and E. A. Lombardo. J. Catal., 70, 356 - 363 (1981).
8. N. Tien-Thao, H. Alamdari, M. H. Zahedi-Niaki, S. Kaliaguine. J. Catal. 245 (2007) 346-357.
9. J. A. B. Bourzutschky, N. Homs and A. T. Bell. J. Catal., 124, 52 -72 (1990).
10. S. Kaliaguine, A. Van Neste, V. Szabo, J. E. Gallot, M. Bassir, R. Muzychuk. Appl. Catal. A 209, 345 - 458 (2001).
11. H. P. Klug and L. E. Alexander. Procedures for polycrystalline and amorphous materials, John Wiley & Sons, New York/London (1962).
12. T. Ito, Q. Zhang, F. Saito. Powder Technol., 143-144, 170 - 173 (2004).
13. S. Royer, A. Van Neste, R. Davidson, S. McIntyre and S. Kaliaguine. Ind. Eng. Chem. Res. 43, 5670 - 5680 (2004).
14. N. Tien-Thao, H. Alamdari, S. Kaliaguine. J. Solid State Chem., 181, 2006 - 2019 (2008).
15. S. M. Lima, J. M. Assaf, M. A. Pena, J. L. G. Fierro. Appl. Catal. A, 311, 94 - 104 (2006).
16. M. Xu, M. J. L. Gines, A. -M. Hilmen, B. L. Stephens and E. Iglesia. J. Catal., 171, 130 - 147 (1997).
17. R. D. S. Monteiro, F. B. Noronha, L. C. Dieguez, M. Schmal. Appl. Catal., 131, 89 - 106 (1995).
18. N. W. Hurst, S. J. Gentry and A. Jones. Catal. Rev.-Sci. Eng., 24, 233 - 309 (1982).
19. J. A. Marcos, R. H. Buitrago and E. A. Lombardo. J. Catal., 105, 95 - 106 (1987).
20. R. Lago, G. Bini, M. A. Peña and J. L. G. Fierro. J. Catal., 167, 198 - 209 (1997).

